

## Assignment of the Raman lines in single crystal barium metaborate ( $\beta$ -BaB<sub>2</sub>O<sub>4</sub>)

This article has been downloaded from IOPscience. Please scroll down to see the full text article.

1998 J. Phys.: Condens. Matter 10 673

(<http://iopscience.iop.org/0953-8984/10/3/018>)

View [the table of contents for this issue](#), or go to the [journal homepage](#) for more

Download details:

IP Address: 171.66.16.209

The article was downloaded on 14/05/2010 at 12:00

Please note that [terms and conditions apply](#).

## Assignment of the Raman lines in single crystal barium metaborate ( $\beta$ -BaB<sub>2</sub>O<sub>4</sub>)

P Ney<sup>†</sup>, M D Fontana<sup>†</sup>, A Maillard<sup>†</sup> and K Polgár<sup>‡</sup>

<sup>†</sup> Laboratoire Matériaux Optiques à Propriétés Spécifiques, CLOES, Université de Metz et Supélec, 2 rue E Belin, 57078 Metz Cedex 3, France

<sup>‡</sup> Research Laboratory for Crystal Physics, Hungarian Academy of Sciences, Budaörsi út 45, H-1112 Budapest, Hungary

Received 27 January 1997, in final form 9 September 1997

**Abstract.** A Raman-scattering study performed on  $\beta$ -BaB<sub>2</sub>O<sub>4</sub> ( $\beta$ -BBO) at room temperature allows us to assign all the vibrational modes detected in the Raman spectra. The internal and external vibration modes are properly obtained by taking account of the light polarization, mode contamination and isotope effects. A correspondence between the lattice and the free-ring modes is also presented.

### 1. Introduction

Barium metaborate ( $\beta$ -BaB<sub>2</sub>O<sub>4</sub> or  $\beta$ -BBO) is known to be an excellent nonlinear optical material [1–3] with a wide transmission range 189–3500 nm and a high damage threshold (15 GW cm<sup>-2</sup>). It should be of special interest in studying the origin and the microscopical mechanism of the nonlinear optical properties in borates, particularly in  $\beta$ -BBO. The Raman spectrum can provide useful information for it. This requires a proper assignment of all Raman lines and the knowledge of the frequency and the corresponding ionic motion for each phonon. Here we are concerned by this objective.

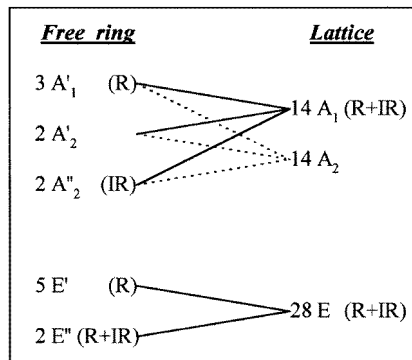
Only a few papers have been published about the Raman and infrared (IR) spectra at room temperature [4–6]. They revealed discrepancies about the mode assignments in the crystal. In this paper, we present the whole Raman spectrum recorded at room temperature for various configurations and we assign all Raman lines. For this, we account for the influence of the light polarization as well as the possible effects of mode contamination and the isotopes in the Raman spectra. Finally, a link is established in the frequencies and ionic motions between the crystal lattice and the free metaborate ring (B<sub>3</sub>O<sub>6</sub>)<sup>3-</sup>.

The disagreements reported between the previous investigations are shown to arise from the leakage of A<sub>1</sub> mode in the E spectra, the nonconsideration of the isotopic effect and the strong variation of the polarizability between different configurations.

### 2. Symmetry analysis

The rhombohedral unit cell of  $\beta$ -BBO contains six BaB<sub>2</sub>O<sub>4</sub> molecules corresponding to four (B<sub>3</sub>O<sub>6</sub>)<sup>3-</sup> anionic groups (site symmetry C<sub>3</sub>) and six Ba<sup>2+</sup> cations (site symmetry C<sub>1</sub>). The anionic groups are perpendicular to the polar axis and ionically bonded through the barium cations Ba<sup>2+</sup> [1, 7]. The  $\beta$ -BBO crystal belongs to the C<sub>3v</sub><sup>6</sup> space group and the

**Table 1.** Correlation between the modes in the free ring and in the crystal. R and IR denote the Raman and infrared activity respectively.



irreducible representations of the normal modes at the zone centre can be separated in two contributions:

- the modes arising from internal vibrations of the 'free' metaborate ring according to

$$\Gamma_{\text{int}} = 14A_1 + 14A_2 + 28E$$

- the modes corresponding to librations or translations of metaborate ring and of barium cations

$$\Gamma_{\text{ext}} = 6A_1 + 7A_2 + 13E$$

where both the  $A_1$  and  $E$  species are Raman and IR active.

The Raman tensors for the  $C_{3v}^6$  point group are written as

$$A_1(z) = \begin{vmatrix} a & 0 & 0 \\ 0 & a & 0 \\ 0 & 0 & b \end{vmatrix} \quad E(x) = \begin{vmatrix} 0 & c & d \\ c & 0 & 0 \\ d & 0 & 0 \end{vmatrix} \quad E(y) = \begin{vmatrix} c & 0 & 0 \\ 0 & -c & d \\ 0 & d & 0 \end{vmatrix}.$$

The point-group symmetry of the 'free' or isolated metaborate ring  $(B_3O_6)^{3-}$  is  $D_{3h}$  and the corresponding irreducible representations of the normal modes are given at the zone centre by

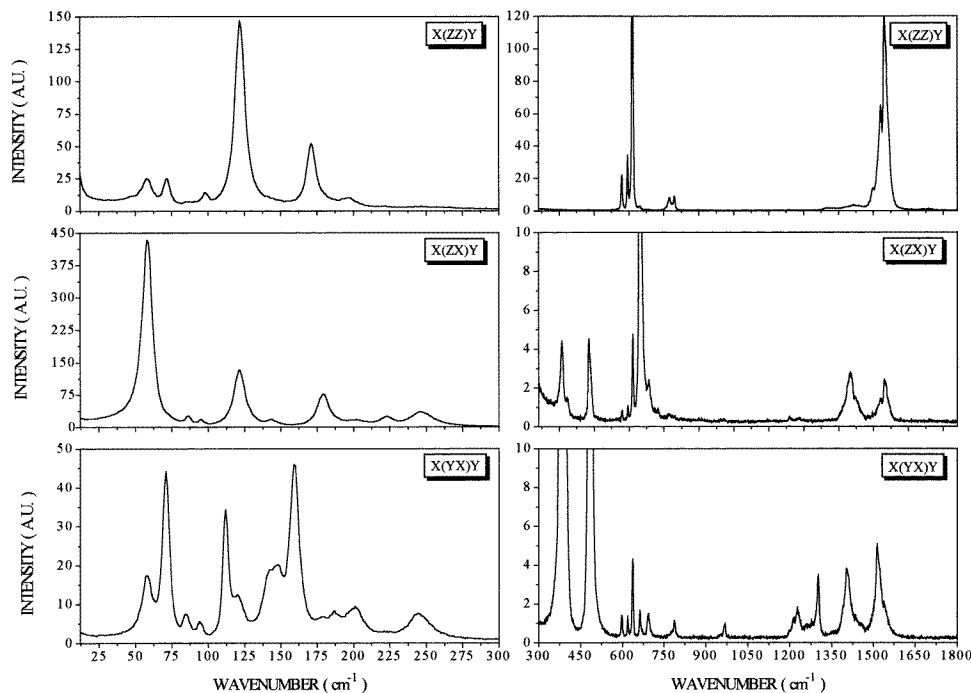
$$\Gamma_{\text{ring}} = 3A_1' + 2A_2' + 2A_2'' + 5E' + 2E''.$$

The correspondence between modes in the free ring and those in the lattice is established in table 1. For this, we use the fact that each vibrational mode of the 'free'  $(B_3O_6)^{3-}$  anions splits into components in the crystal owing to the effect of lattice correlation [4–6].

### 3. Experimental results and assignment of the vibrational modes

$\beta$ -BBO single crystal was grown by the top seeding solution growth (TSSG) technique from a solution containing  $BaB_2O_4$  and  $BaB_2O_4 \cdot Na_2O$  [8]. The seed was oriented along the crystallographic axis  $c = [0001]$ , the pulling rate was 0.2 mm/day with five rotations/min. A  $4 \times 4 \times 4.7$  mm<sup>3</sup> sample was prepared using standard mechanical cutting and polishing methods and x-ray oriented with a precision of 0.5°. The standard set of orthogonal principal axes  $X, Y, Z$  is chosen parallel to the trigonal axes  $a, b \perp a, c$ .

The Raman spectra of the  $\beta$ -barium metaborate crystal are recorded at room temperature with the 514.5 nm Ar<sup>+</sup> laser line (400 mW) as the exciting line and by means of a SPEX



**Figure 1.** Raman spectra in  $\beta$ -BBO at room temperature in various scattering geometries corresponding to  $A_1$  [ $X(ZZ)Y$ ],  $E_x(d)$  [ $X(ZX)Y$ ] and  $E_x(c)$  [ $X(YX)Y$ ] modes. Note the change in the intensity scale whereas the spectra are recorded in the same experimental conditions.

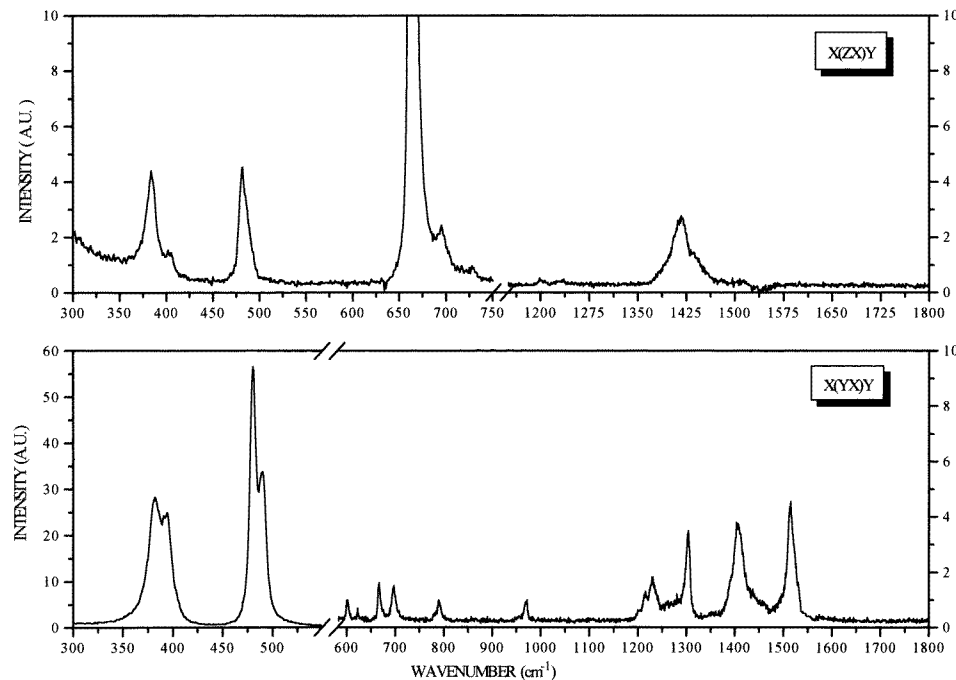
1401 double-grating spectrometer. The right-angle geometry is used to study Raman spectra in the range 0–1600  $\text{cm}^{-1}$ . Three spectra recorded in different configurations under the same experimental conditions are presented in figure 1.

The spectra were recorded in the geometries  $X(ZZ)Y$ ,  $X(ZX)Y$  and  $X(YX)Y$  where the notation stands for the  $A_1(b)$ ,  $E(d)$  and  $E(c)$  modes respectively and where the letters in parentheses represent the corresponding components of the polarizability tensor.

As the short-range interatomic forces predominate over long-range electrostatic forces in  $\beta$ -BBO, the splitting between the  $A_1$  and  $E$  symmetry modes is expected to be much larger than the LO–TO frequency splitting. Consequently, for  $A_1$  and  $E$  species, the TO and LO components overlap and are nearly at the same frequencies [9].

The spectra are divided into two well-defined parts. The low frequency (0–300  $\text{cm}^{-1}$ ) lines are related to the external modes whereas the high frequency (300–1600  $\text{cm}^{-1}$ ) peaks are linked to the internal vibrational modes of the metaborate ring.

The  $A_1$  spectrum displays intense peaks in the high-frequency range, which are much larger than those measured in the  $E$  spectra. As a consequence, even a small misorientation of the polarizers or the sample leads to a leakage of  $A_1$  modes in the less intense  $E$  spectrum. Indeed, we have calculated that a 2% leakage of the  $A_1$  mode intensity is sufficient to explain their detection in the  $E$  spectrum. Therefore, some  $A_1$  lines have the same intensities as those exhibited by some  $E$  peaks. Consequently, the  $E$  spectra have to be corrected to account for the contamination arising from  $A_1$  modes. Corrected high-frequency  $E$  spectra are shown in figure 2.



**Figure 2.** *E* symmetry spectra after the correction due to the  $A_1$  mode contamination.

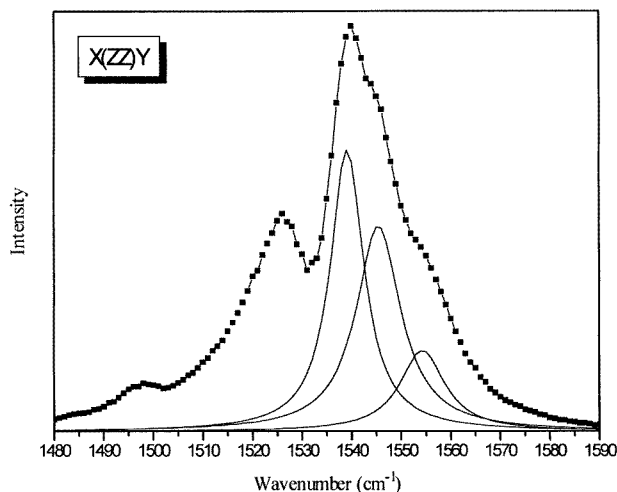
According to group theory, the spectra recorded in  $X(ZX)Y$  and  $X(YX)Y$  scattering geometries are expected to yield the same *E* modes. However both spectra strongly differ in shape and in intensity for low- and high-frequency ranges. In fact, they provide the same frequencies but with completely different intensities. This is particularly observed in the intensity scales used for the low-frequency range. This feature could be due to a large change in the polarizability between the *d* and *c* components and thus be related to the different internal motions of the crystal. Indeed the  $E(d)$  modes detected in the  $X(ZX)Y$  scattering correspond to out-of-plane motions whereas the  $E(c)$  modes seen in the  $X(YX)Y$  geometry arise from in-plane vibrations.

Now we focus our attention on the  $A_1$  lines in the high-frequency range between 1300 and 1600  $\text{cm}^{-1}$  (see figure 1(a)). The broad bands around 1332 and 1421  $\text{cm}^{-1}$  were attributed to two-phonon processes [5, 9].

The spectrum shown in figure 3, recorded between 1480 and 1590  $\text{cm}^{-1}$ , reveals the presence of five unambiguous lines. After a first approach based on the frequencies of these Raman peaks, we attribute them to the isotopic effect.

In fact, we linked this effect to the presence of two boron isotopes  $^{10}\text{B}$  and  $^{11}\text{B}$  and which is able to split the lines according to the mass of the various formula of the metaborate ring, i.e.  $^{10}\text{B}_3\text{O}_6$ ,  $^{10}\text{B}_2^{11}\text{BO}_6$ ,  $^{10}\text{B}^{11}\text{B}_2\text{O}_6$  and  $^{11}\text{B}_3\text{O}_6$ . As the vibrational mode frequency depends on the mass, this effect is expected to be larger for high frequency peaks. Consequently, the  $A_1'$  line of the free metaborate ring at 1528  $\text{cm}^{-1}$  leads to two lines in the crystal, each of them giving rise to four peaks due to the isotopic effect.

In the highest frequency group, between 1530 and 1590  $\text{cm}^{-1}$ , if we assume that the heaviest structure  $^{11}\text{B}_3\text{O}_6$  corresponds to the lowest frequency line at 1539  $\text{cm}^{-1}$ , we can calculate the position expected for the other peaks by using the mass of each metaborate ring.



**Figure 3.** Splitting of two  $A_1$  (TO) modes into five lines, owing to the isotopic effect. The experimental data are represented by squares whereas the continuous line is the least squares fit obtained by using damped harmonic oscillators.

**Table 2.** Assignment of the Raman lines to the vibrational modes. The upper index 'is' denotes the mode splitting due to the isotopic effect.

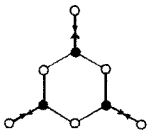

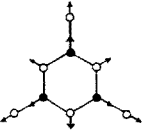
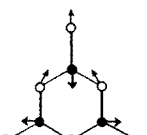
Modes		Frequency ( $\text{cm}^{-1}$ )
$A_1$	External	58 - 72 - 98 - 122 - 171 - 195
	Internal	599 <sup>is</sup> - 620 <sup>is</sup> - 637 - 770 - 787 - 1497 <sup>is</sup> - 1525 <sup>is</sup> - 1539 <sup>is</sup> - 1545 <sup>is</sup> - 1554 <sup>is</sup>
E	External	58 - 71 - 86 - 95 - 112 - 120 - 143 - 148 - 159 - 187 - 202 - 222 - 245
	Internal	180 - 382 - 395 - 481 - 491 - 663 - 695 - 725 - 969 - 1200 - 1214 - 1227 1305 - 1405 - 1417 - 1437 - 1514

We obtain, for the formulae  $^{10}\text{B}^{11}\text{B}_2\text{O}_6$  and  $^{10}\text{B}_2^{11}\text{BO}_6$  the frequencies at 1545 and 1551 respectively, which are in good agreement with the values at 1545 and 1554  $\text{cm}^{-1}$  derived from the fit of the spectrum. The fourth line (calculated at 1557  $\text{cm}^{-1}$ ) corresponding to the rarest  $^{10}\text{B}_3\text{O}_6$  group was not detected because its intensity is too low.

For the low-frequency group of lines between 1490 and 1530  $\text{cm}^{-1}$  and according to the mass of the isotopic groups, Raman lines are expected at 1527, 1521, 1515 and 1509  $\text{cm}^{-1}$  whereas only peaks at 1525 and 1497  $\text{cm}^{-1}$  are clearly detected. Lines at 1521 and 1515  $\text{cm}^{-1}$  are probably hidden in the low frequency tail of the intense peak at 1525  $\text{cm}^{-1}$ .

This study is not complete, because it is difficult to extract more results from our data, but is sufficient to explain the splitting of the Raman lines between 1480 and 1590  $\text{cm}^{-1}$ .

Table 3. Lattice and free-ring modes and the corresponding ionic motions.

Free ring vibrations		Frequencies in crystal (our results)	
Internal motion in free ( $B_3O_6$ )	Mode, frequency, main motions	(correlation effect)	(isotopic effect)
	Mode : $A'_1$ $\nu_1 = 1528 \text{ cm}^{-1}$ stretching vibrations of extra-ring B-O' bonds	Mode symmetry : $A_1$ 1525 $\text{cm}^{-1}$ 1545 $\text{cm}^{-1}$	1497, 1525 $\text{cm}^{-1}$ 1539, 1545, 1554 $\text{cm}^{-1}$
	Mode : $A'_1$ $\nu_2 = 773 \text{ cm}^{-1}$ stretching vibrations of intra-ring B-O bonds	Mode symmetry : $A_1$ 770 $\text{cm}^{-1}$ 787 $\text{cm}^{-1}$	
	Mode : $A'_1$ $\nu_3 = 639 \text{ cm}^{-1}$ intra-ring angle-bending	Mode symmetry : $A_1$ 610 $\text{cm}^{-1}$ 637 $\text{cm}^{-1}$	599, 620 $\text{cm}^{-1}$
	Mode : $E'$ $\nu_8 = 1408 \text{ cm}^{-1}$ stretching of the extra-ring B-O' bonds	Mode symmetry : $E(c)$ 1405 $\text{cm}^{-1}$ 1417 $\text{cm}^{-1}$ 1437 $\text{cm}^{-1}$ 1514 $\text{cm}^{-1}$	


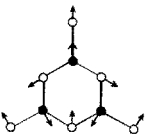
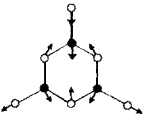
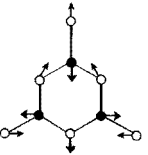
By taking into account the previous remarks, we attempt to assign the Raman lines to vibrational modes in  $\beta$ -BBO and the results are reported in table 2.

These results are in good agreement with those deduced from IR reflectivity measurements [4, 10].

We note that the total number of external modes ( $6A_1 + 13E$ ) is obtained as expected by group theory. In contrast, some lines are missing for internal vibrational modes. In fact, if we do not account for the isotope effect, only the six  $A_1$  lines arising from the three  $A'_1$  modes of the free ring were detected and listed on table 2. The  $A_1$  lines coming from Raman inactive  $A'_2$  and  $A''_2$  modes were not observed, probably because their intensity is too low.

Now we associate each mode to the corresponding ionic motion. For this, we use the calculated frequencies for the vibrations of the free metaborate ring [5, 10, 11] to assign the origin of the lines detected in our Raman spectra. The results are shown in table 3.

Table 3. (Continued)

<u>Free ring vibrations</u>		<u>Frequencies in crystal (our results)</u>
<i>Internal motion in free (B<sub>3</sub>O<sub>3</sub>)</i>	<i>Mode, frequency, main motions</i>	<i>(correlation effect)</i>
	Mode : E' $\nu_9 = 1227 \text{ cm}^{-1}$ stretching of the intra-ring B-O bonds	Mode symmetry : E(c) 1214 $\text{cm}^{-1}$ — — 1227 $\text{cm}^{-1}$
	Mode : E' $\nu_{10} = 971 \text{ cm}^{-1}$ stretching of the intra-ring B-O bonds	Mode symmetry : E(c) 969 $\text{cm}^{-1}$ — — —
	Mode : E' $\nu_{11} = 480 \text{ cm}^{-1}$ intra-ring angle-bending	Mode symmetry : E(c) 479 $\text{cm}^{-1}$ 481 $\text{cm}^{-1}$ 488 $\text{cm}^{-1}$ 491 $\text{cm}^{-1}$
	Mode : E' $\nu_{12} = 380 \text{ cm}^{-1}$ intra-ring angle bending + B-O stretching	Mode symmetry : E(c) 382 $\text{cm}^{-1}$ 391 $\text{cm}^{-1}$ 395 $\text{cm}^{-1}$ —

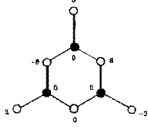
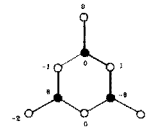
#### 4. Conclusion

If compared with the results reported in the literature, our assignment of the Raman lines is more complete and differs from previous studies about some lines. One of the reasons is related to the crystal symmetry used in this analysis. The symmetry of the low-temperature structure of BBO was given by Lu *et al* [12] as  $R3 (C_3^4)$  and then by Liebertz and Stähr [13] as  $R3c (C_{3v}^6)$ . This symmetry was later confirmed by Eimerl *et al* [1] and by Fröhlich [14].

Since they assumed  $C_3^4$  symmetry, most of the previous Raman studies [9–11] present contradictions with the investigations based upon the  $C_{3v}^6$  symmetry [4–6]. Nevertheless, these three last papers exhibit some errors in the assignments of the modes. Raman and IR



Table 3. (Continued)

Free ring vibrations		Frequencies in crystal (our results)
Internal motion in free ( $B_3O_6$ )	Mode, frequency, main motions	(correlation effect)
	Mode : $E''$ $\nu_{13} = 665 \text{ cm}^{-1}$ out-of plane vibration	Mode symmetry : $E(d)$ 663 $\text{cm}^{-1}$ — — 695 $\text{cm}^{-1}$
	Mode : $E''$ $\nu_{14} = 186 \text{ cm}^{-1}$ out-of plane vibration	Mode symmetry : $E(d)$ 180 $\text{cm}^{-1}$ — — —

spectra were used in [4] to assign the vibrational modes, but the lack of Raman measurements related to the  $xy$ ,  $yx$ ,  $xx$ ,  $yy$  components of the polarizability tensor led to an incorrect assignment of some lines. In [5], the Raman study was carried out with nonpolarized light and restricted to the range 350–1800  $\text{cm}^{-1}$  so that not all the vibrational modes were determined. Finally, the authors of [6] reported various assignments and TO–LO splittings among the  $E$  lines whereas it is known that all the TO and LO of both  $A_1$  and  $E$  modes are overlapped in the spectra.

A Raman scattering study, performed at room temperature has provided the assignment of all the vibrational modes detected in the Raman spectra. The number of external modes was obtained in agreement with the theoretical analysis and all the Raman lines between 300 and 1600  $\text{cm}^{-1}$  were properly assigned although the expected number of modes was not found. We have also showed that the isotopic effect is responsible for the splitting of some high-frequency lines. Further, we have reported the ionic motions associated with the main internal modes using the correspondence between the lattice modes and the modes in the free ring.

### Acknowledgment

This research was supported by the Scientific Research Foundation of Hungary under project OTKA T-014026.

### References

- [1] Eimerl D, Davis L, Velsko S, Graham E K and Zalkin A 1987 *J. Appl. Phys.* **62** 1968
- [2] Kozuki Y and Itoh M 1991 *Nonlinear Opt.* **1** 187
- [3] Nikogosyan 1991 *Appl. Phys. A* **52** 359
- [4] Hong S L and Wu B C 1995 *Opt. Eng.* **34** 1738

- [5] Voron'ko Y K, Gorbachev A V, Sobol' A A and Tsymbal L I 1994 *Inorg. Mater.* **30** 603
- [6] Roussigné Y, Farhi R and Dugautier C 1992 *Solid State Commun.* **82** 287
- [7] Mighell A D, Perloff A and Block S 1966 *Acta Crystallogr.* **20** 819
- [8] Polgár K and Péter A 1993 *J. Cryst. Growth* **134** 219
- [9] Lu J Q, Lan G X, Li B, Yang Y Y, Wang H F and Wu B C 1988 *J. Phys. Chem. Solids* **49** 519
- [10] Tian B, Wu G and Xu R 1987 *Spectrochim. Acta* **43A** 65
- [11] Wang Y F, Lan G X and Wang H F 1992 *Spectrochim. Acta* **48A** 181
- [12] Lu S, Ho M and Huang J 1982 *Acta Phys. Sin.* **31** 948
- [13] Liebertz J and Stähr S 1983 *Z. Kristallogr.* **165** 91
- [14] Fröhlich R 1984 *Z. Kristallogr.* **168** 109